# EFFECTS OF UNSUPERVISED FULLY CONSTRAINED LEAST SQUARES LINEAR SPECTRAL MIXTURE ANALYSIS METHOD ON AUTOMATIC CLASSIFICATION OF TM IMAGE

Hong-xia LUO [a, b,*], Jianya GONG[a], Jianping PAN [a]

a State Key Laboratory of Information Engineering in Surveying, Mapping and Remote Sensing ,Wuhan University, 129 Luoyu Road, wuhan. Hubei, China-geogjy@163.net
b School of Resources and Environment, Southwest Normal University, 2 Tiansheng Road, Chongqing, China - tam_7236@swnu.edu.cn

**KEY WORDS:** classification of remote sensing image, linear spectral mixture model, fully constrained least squares (FCLS) algorithm, unsupervised FCLS (UFCLS) method, constrained optimization problem

**ABSTRACT:**

Statistical analysis is a widely used traditional technique for classification and discrimination in remotely sensed images, which supposes that there is only one endmember in an image pixel. However, the fact is that the ground sampling distance is generally larger than the size of targets of interest. So the statistical analysis technique is not suitable. In this case, classification and discrimination must be carried out at subpixel level. In this paper the abundance fractions of endmembers in an image pixel are estimated by UFCLS (unsupervised fully constrained least squares) method based on the inversion of linear spectral mixture model. This method allows us to extract necessary endmember information from an unknown and no prior knowledge image scene so that the endmembers present in the image can be quantified. The pixel classification generates a gray scale image, whose gray level values are determined by the estimated abundance fractions of endmembers. The band expansion technique is used to create additional bands from existing multispectral bands using band-to-band nonlinear correlation. These expanded bands ease the problem of insufficient bands in TM imagery. In the two experiments, the results of the pixel classification show that the effects are good. The pixel classification image of vegetation agrees significantly with the NDVI image, but the contrast of the former is a little larger than that of the latter, so there was lack of the information of details and edges. However, compared to color composite image of raw bands 4, 3 and 2 in red, green and blue respectively, especially in the second experiment, the results of vegetation classification are excellent. The shade areas in the first experiment are not classified correctly. Compared to CSMA (constrained spectral mixture analysis) method, UFCLS method is better in both the effects of classification and the consumption of computation time.

## 1. INTRODUCTION

Statistical analysis such as maximum likelihood, minimum distance and mahalanobis distance, is a widely used traditional technique for classification and discrimination in remotely sensed images, which differentiates pixel one by one according to the average spectral signature of materials, is a classification method of pure pixel discrimination. These traditional statistical classification and discrimination methods suppose that there is only one endmember in an image pixel. However, the fact is that a pixel is generally mixed by a number of endmembers in the image given spatial resolution. Consequently, mixed pixel analysis techniques such as spectral mixture model have been proposed to describe such mixing activities. The mixed pixel classification generally generates a gray scale image whose gray level values are determined by the estimated abundance fractions of the endmembers resident in the image pixels. Although there are many spectral mixture models, they all belong to two classes, linear and nonlinear models respectively. To this day, the linear spectral mixture model is favorably received and most widely used. Its prominent characteristic is very simple. It was reported by Zhao Ying-shi (2001) that the linear spectral mixture model was better than the tasseled cap transformation when used to extract sands information.

Currently, the approach mostly used to decompose the mixed pixels by linear model, also be called model inversion, is the least squares method. If considering it from the point of minimizing the merit function, this is a constrained optimization problem because the parameters of the linear model generally have explicit physical meaning and constraints. The optimization algorithms include the regularly searching algorithms such as downhill simplex, conjugate direction set and passive set, and the randomly searching algorithms proposed in the recent years such as GA (genetic algorithm), ES and EP. However, the latter is not better than the former for the inversion of the linear spectral mixture model, and cost longer computation time (Tang Shihao et al., 2002). The regularly searching algorithms are frequently used in the inversion of remote sensing models currently. Unsupervised fully constrained least squares (UFCLS) recently proposed by Daniel et al. (2001) improved the computation speed, which applied the method based on the least squares and resembling the passive set of the regularly searching algorithms. Under the circumstance without prior knowledge, this method is valid for decomposing mixed pixels in remote sensing images. In this paper, we analyze the effects of UFCLS on classification of TM image.

* Correspondence to: Hong-xia LUO

## 2. LINEAR SPECTRAL MIXTURE MODEL

The linear spectral mixture model is a mostly simple and widely used approach for remotely sensed imagery to estimate abundance fractions of the endmembers resident in the mixed pixels. Suppose that $L$ is the number of spectral bands. Let $\boldsymbol{D_N}$ be an $L\times1$ column pixel vector in a multispectral or hyperspectral image. Let $\boldsymbol{M}$ be an $L\times p$ endmember signature matrix denoted by $[\mathbf{m}_1\ \mathbf{m}_2\ \dots\ \mathbf{m}_p]$ where $\mathbf{m}_j$ is an $L\times1$ column vector represented by the signature of the j-th endmember and $p$ is the number of endmembers in the image scene. Let $\alpha=[\alpha_1\ \alpha_2\ \dots\ \alpha_p]^T$ be a $p\times1$ abundance column vector associated within $\boldsymbol{D_N}$, where $\alpha_j$ denotes the fraction of the j-th signature present in the pixel vector $\boldsymbol{D_N}$ .A linear mixture model of $\boldsymbol{D_N}$ makes use of a mixing equation to model the spectral signature of $\boldsymbol{D_N}$ as a linear combination of $\mathbf{m}_1\ \mathbf{m}_2\ \dots\ \mathbf{m}_p$ with appropriate abundance fractions specified by $\alpha_1\ \alpha_2\ \dots\ \alpha_p$ as follows.

$$D_N=M\alpha+E \tag{1}$$

Where $\boldsymbol{E}$ is noise or can be interpreted as measurement error. Here, $\boldsymbol{D_N}$ will be used to represent digital numbers. In general, two constraints must be imposed on this model to yield an optimal solution. These are the abundance sum-to-one constraint (ASC), $\sum_{j=1}^{p}\alpha_j=1$ and the abundance nonnegativity constraint(ANC), $\alpha_j\geq0$ for all $1\leq j\leq p$.

## 3. UFCLS METHOD

### 3.1 FCLS Algorithm

FCLS algorithm is introduced firstly in order to understand UFCLS method, because of the latter derived from the former. FCLS is the abbreviation of *fully constrained least squares*, namely, the late is the algorithm about the inversion of $\alpha$ in the equation(1) when two constraints, ASC and ANC, must be imposed on it at the same time. Taking care of the ASC, we introduce a new signature matrix, denoted by $\boldsymbol{N}$, and a vector $\boldsymbol{S}$, defined respectively by

$$\boldsymbol{N}=\begin{bmatrix}\delta\mathrm{M}\\ \boldsymbol{I}^T\end{bmatrix}\quad \text{with } \boldsymbol{I}=\underbrace{(1,1,\cdots1)}_{p}^{\mathrm{T}} \tag{2}$$

$$\boldsymbol{S}=\begin{bmatrix}\delta\boldsymbol{D}_N\\ 1\end{bmatrix} \tag{3}$$

The utilization of $\delta$ in (2), (3) controls the impact of the ASC. In this paper, the value of $\delta$ was fixed at $1.0\times10^{-5}$.

If the $\boldsymbol{M}$ and $\boldsymbol{D_N}$ in (1) are replaced with $\boldsymbol{N}$, $\boldsymbol{S}$ respectively, the equation can be derived as

$$S=N\alpha+\mathrm{n} \tag{4}$$

It is the solution of the equation (4) that satisfies the above ASC condition. In the equation (4), the values of $\boldsymbol{D_N}$ are known in a given image, and the values of $\boldsymbol{M}$ are supposed to be known, so the values of $\boldsymbol{N}$ and $\boldsymbol{S}$ are known. Consequently, solving $\alpha$ becomes to solve p unknown parameters from L+1 equations. We use the least squares error as the optimal least squares estimate of $\alpha$ , $\alpha_{\mathrm{LS}}$, for equation (4) can be obtained by

$$\alpha_{\mathrm{LS}}=(\boldsymbol{N}^{\mathrm{T}}\boldsymbol{N})^{-1}\boldsymbol{N}^{\mathrm{T}}\boldsymbol{S} \tag{5}$$

Next, we impose ANC on model (4). Under the constraint, the equation (4) can not be solved analytically since ANC results in a set of inequalities, only an optimal solution can be obtained, which generates the following constrained optimization problem as

$$\text{Minimize LSE}=(\boldsymbol{N}\alpha-\boldsymbol{S})^{\mathrm{T}}(\boldsymbol{N}\alpha-\boldsymbol{S})\ \text{ s.t. }\alpha\geq0 \tag{6}$$

Many methods have been developed to address this problem. In this section, we use the FCLS method, the principles of which have been described by Daniel et al. (2001) and Bro et al. (1997), the details of implementing the FCLS algorithm are given below.

1. Initialization: The components of the estimate $\alpha_{\mathrm{LS}}$ are decomposed into two index sets called active set and passive set. While the former consists of all indices corresponding to negative (or zero) components in the estimate $\alpha_{\mathrm{LS}}$, the latter contains all indices corresponding to positive components in the estimate $\alpha_{\mathrm{LS}}$. Set the passive set $\mathrm{P}^{(0)}=\{1,2,\dots\mathrm{p}\}$ and active set $\mathrm{R}^{(0)}=\text{ø}$, $k$=0.

2. Calculate $\alpha_{\mathrm{LS}}$ using (5). Let $\alpha_{FCLS}^{(k)}=\alpha_{\mathrm{LS}}$.

3. At the $k$-th iteration, if all components in $\alpha_{FCLS}^{(k)}$ are nonnegative, the algorithm is terminated. Otherwise, continue.

4. Let $k=k+1$. Move all indices in $\mathrm{P}^{(k-1)}$ that correspond to negative (or zero) components of $\alpha_{FCLS}^{(k)}$ to $\mathrm{R}^{(k-1)}$, and the resulting index sets are denoted by $\mathrm{P}^{(k)}$ and $\mathrm{R}^{(k)}$, respectively. Create a new index set $\mathrm{I}^{(k)}$ and set $\mathrm{I}^{(k)}=\mathrm{R}^{(k)}$.

5.Let $\alpha_{\mathrm{R}^{(k)}}=(\alpha_{\mathrm{LS(i)}}\ \alpha_{\mathrm{LS(j)}}\ \dots\ \alpha_{\mathrm{LS(n)}})^{\mathrm{T}}$ , $\alpha_{\mathrm{LS(i)}}$、$\alpha_{\mathrm{LS(j)}}$、…、$\alpha_{\mathrm{LS(n)}}$ are all the components of $\alpha_{\mathrm{LS}}$ in $\mathrm{R}^{(k)}$.

6. Form a steering matrix $\Gamma_{\alpha}^{(k)}$ by deleting all rows and columns in the matrix $(\boldsymbol{N}^{\mathrm{T}}\boldsymbol{N})^{-1}$ that are specified by $\mathrm{P}^{(k)}$.

7. Calculate $\beta^{(\mathrm{k})}=(\Gamma_{\alpha}^{(k)})^{-1}\alpha_{\mathrm{R}^{(\mathrm{k})}}$.If all components in $\beta^{(\mathrm{k})}$ are negative, go to step 12. Otherwise, continue.

8. Calculate $\beta_{\max}^{(k)}=\arg\{\max\beta_j^{(k)}\}$ and move the index in $\mathrm{R}^{(k)}$ that corresponds to $\beta_{\max}^{(k)}$ to $\mathrm{P}^{(k)}$.

9. Form another new matrix $\Upsilon_{\beta}^{(k)}$ by deleting all columns of $(\boldsymbol{N}^{\mathrm{T}}\boldsymbol{N})^{-1}$ specified by $\mathrm{P}^{(k)}$.

10. Recalculate $\beta^{(\mathrm{k})}=(\Gamma_{\alpha}^{(k)})^{-1}\alpha_{\mathrm{R}^{(\mathrm{k})}}$ according to the changed $\mathrm{R}^{(k)}$, then calculate $\alpha_{\mathrm{I}^{(\mathrm{k})}}=\alpha_{\mathrm{LS}}-\Upsilon_{\beta}^{(k)}\beta^{(\mathrm{k})}$.

11. If any components of $\alpha_{1}^{(k)}$ in $I^{(k)}$ are negative, then move corresponding indices from $P^{(k)}$ to $R^{(k)}$. Go to step 5.

12. Form another new matrix $\Upsilon_{\beta}^{(k)}$ by deleting all columns of $(N^{T}N)^{-1}$ specified by $P^{(k)}$.

13. Calculate $\alpha_{FCLS}^{(k)} = \alpha_{LS} - \Upsilon_{\beta}^{(k)} \beta^{(k)}$ and go to step 3.

### 3.2 UFCLS Method

The above FCLS method requires a complete knowledge of the endmember signature matrix ***M***. For the situation of no a *priori* information, it needs an unsupervised process to generate the desired endmember information, based on which the UFCLS method was proposed.

The least squares error (LSE) is a criterion to judge the fit between data measurements and estimated values stand or fall. In the inversion of linear spectral mixture model, we expect to minimize the LSE, i.e., estimated values are extremely close to the data measurements. The UFCLS method makes the endmember signature values to be obtained directly from the remote sensing image iteratively. In every iteration, we judge a pixel to be an endmember pixel or not by the LSE, and decide whether to regard its digital values as endmember signature values. The idea can be described as follows.

Initially, we can select any arbitrary pixel vector as an initial desired endmember $\mathbf{m_0}$. However, a good choice may be the pixel vector with the maximum length $d$ ( $d = \sqrt{\sum_{i=1}^{l} b_i^2}$ , $b_i$ denotes the digital values of the *i*-th band, *l* denotes the numbers of bands). We then assume that all pixel vectors in an image scene are pure pixels made up of $\mathbf{m_0}$ with100% abundance. Of course, this is generally not true. So, we find a pixel vector which has the largest LSE between itself and $\mathbf{m_0}$, and select it as the second endmember $\mathbf{m_1}$. Now, we form an endmember signature matrix $\boldsymbol{M}=[\mathbf{m_0}\ \mathbf{m_1}]$. Because the LSE between $\mathbf{m_0}$ and $\mathbf{m_1}$ is the largest, $\mathbf{m_1}$ is most distinct from $\mathbf{m_0}$.The FCLS algorithm is then used to estimate the abundance fractions of $\mathbf{m_0}$ and $\mathbf{m_1}$ denoted by $\alpha_0^{(2)}(D_N)$ and $\alpha_1^{(2)}(D_N)$ for each pixel vector $\boldsymbol{D_N}$ respectively. The superscript indicates the number of the iteration currently being executed. Here $\boldsymbol{D_N}$ is included in the estimated abundance fractions to emphasize that they are functions of $\boldsymbol{D_N}$. According to the principle of the linear spectral mixture model, we are able to use $\alpha_0^{(2)}(D_N)$ and $\alpha_1^{(2)}(D_N)$ to calculate the estimated values $\hat{D}_N = \alpha_0^{(2)}(D_N)\mathbf{m_0} + \alpha_1^{(2)}(D_N)\mathbf{m_1}$. We then calculate the LSE between $\boldsymbol{D_N}$ and $\hat{D}_N$ for all image pixel vectors $\boldsymbol{D_N}$ using the following equation.

$$\mathrm{LSE}^{(k)}(D_N) = \left(D_N - \left[\sum_{i=0}^{k-1}\alpha_i^{(k)}(D_N)m_i\right]\right)^{T}\left(D_N - \left[\sum_{i=0}^{k-1}\alpha_i^{(k)}(D_N)m_i\right]\right) \quad (7)$$

The pixel vector that yields the largest LSE will be selected to be the third endmember $\mathbf{m_2}$. The same procedure of using the FCLS algorithm with $\boldsymbol{M}=[\mathbf{m_0}\ \mathbf{m_1}\ \mathbf{m_2}]$ is repeated until the resulting LSE is small enough and below a given error threshold.

## 4. EXPERIMENTAL RESULTS

### 4.1 Experiment 1

The data used in this section are ETM＋ data, which were obtained on 2 January 2000 over Shenzhen city and the vicinity of it, China. The ETM＋ image consists of eight bands, and we only selected six bands in the visible and infrared spectral region, referred to band 1 to band 5 and band 7. The spatial resolution of the six bands is 30 m. The digital value for every image pixel is constrained from 0 to 255. Because the ETM＋ data which we obtained here were corrected radiometrically and geometrically initially, they were only registered. It is a subscene of 51×51 pixels with few manmade objects for the convenience of analysis extracted from the low right corner of the scene, shown in Fig. 1.

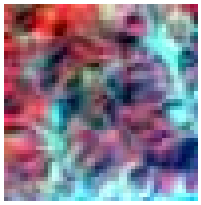

Figure 1. The experiment images of the 51×51 pixels

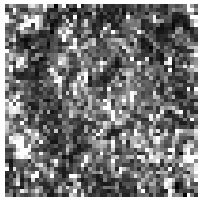

Figure 2.The LSE image of $\mathbf{m_5}$

We know from the linear spectral mixture model(1) that solving $\alpha$ actually becomes to solve ***p*** unknown parameters from ***L*** linear equations if ***M*** and $\boldsymbol{D_N}$ are prior known, which requires ***L*** larger than ***p*** .However, we only selected six bands, so we can solve six unknown parameters at best. For easing the problem of insufficient bands in multispectral imagery, and no prior knowledge on the numbers of endmembers, we expanded six bands to eighteen bands so that there were sufficient bands to calculate iteratively a set of $\mathrm{LSE}_{max}$, the maximum of LSE. The expanded bands were generated by taking the square root of the cross-correlation between band1 and band4, band1 and band5, band1 and band6, band2 and band3, band2 and band 4, band2 and band 5, band2 and band6, band3 and band4, band3 and band 5, band3 and band 6, band4 and band6, and band5 and band6. The square root function was applied to keep the magnitudes of the resulting image pixels similar to the original data.

After 10 iterations using UFCLS method, a set of $\mathrm{LSE}_{max}$ was obtained, shown in Table 1. From the table we see that the $\mathrm{LSE}_{max}$ decreased constantly with the increase of iterative times, first decreased at a high speed, but the more later the iteration came to the more slowly it decreased. There is a distinct borderline at $\mathbf{m_5}$ iteration since after that the $\mathrm{LSE}_{max}$ decreased very slowly, which shows that the extracted pixel vector after it is not endmember but noise. In Fig.2 the LSE image of $\mathbf{m_5}$ also accounts for it. So, in this section the first six extracted pixel vector were selected as endmembers.

| $m_0$ | $m_1$ | $m_2$ | $m_3$ | $m_4$ | $m_5$ | $m_6$ | $m_7$ | $m_8$ | $m_9$ |
|---|---|---|---|---|---|---|---|---|---|
| 50657 | 3809 | 520 | 165 | 118 | 68 | 63 | 61 | 53 | 43 |

Table 1. The LSE of 10 iterations by UFCLS

The six endmembers formed an endmember signature matrix. Then we plugged the endmember signature matrix into (1) to estimate the abundance fractions of the six endmembers using FCLS algorithm for all pixel vectors in the subscene image. The results are shown in Fig.3, where the larger the abundance fractions are, the higher the brightness are shown in the gray scale image, and the smaller the abundance fractions are, the lower the brightness are shown. We know the six endmembers were extracted without prior knowledge from the image using UFCLS method, so which materials can they not be identified to be without true data of the land cover. However we can judge the $\mathbf{m_2}$ endmember to be vegetation directly from the pseudo color image. In order to verify the results, we compare the classification image of vegetation in Fig. 4(a), i.e., the abundance fractions image of $\mathbf{m_2}$, with NDVI in Fig. 4(b). It is shown that the pixel classification image of vegetation agrees significantly with the NDVI image, but the contrast of the former is a little larger than that of the latter, so there is lack of the information of details and edges. It is because the values shown in the two images have different physical meanings, the former denotes the abundance fractions of vegetation, the latter denotes NDVI, which are generally larger than 0 even under the circumstance of non-vegetation. And it is also shown, in Fig. 4(a) denoted by the circle, that the shade areas were not classified correctly.

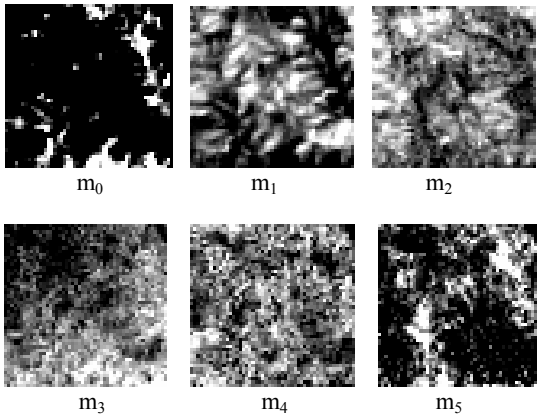


Figure 3. The results of the classification of 6 Endmembers

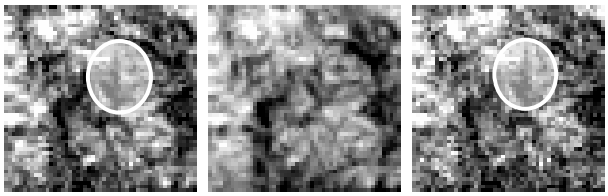

(a)$\mathbf{m_2}$(UFCLS) (b)NDVI (c) $\mathbf{m_2}$ (CSMA)

Figure 4. The effects of the classification of $\mathbf{m_2}$(UFCLS) and $\mathbf{m_2}$ (CSMA) compared to NDVI

### 4.2 Experiment 2

The data considered in this section are TM data with seven bands from Landsat 5, which were obtained on 19 July 1991 located in WRS123/039. Here we selected six bands excluding thermal infrared region. Firstly, the scene was corrected geometrically and registered. A subscene of size 512×512 pixels, larger than the area in experiment 1, was selected from Chibi County, Hubei Province in China for study. A map showing the location of the study area is presented in Fig.5. The color composite image of the study area, of raw bands 4, 3 and 2 in red, green and blue respectively, is shown in Fig.6.

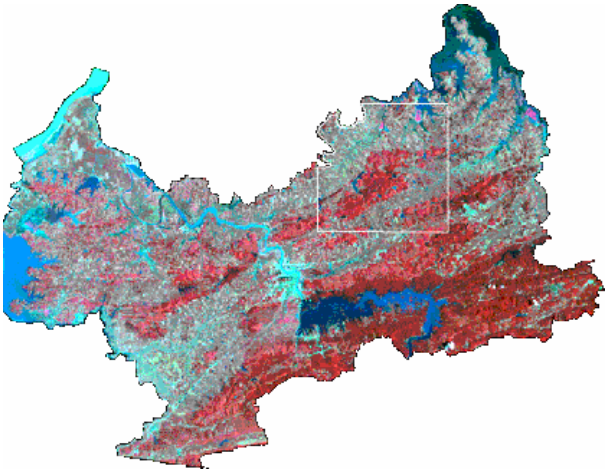

Figure 5. Location of study area in Chibi County, Hubei Province

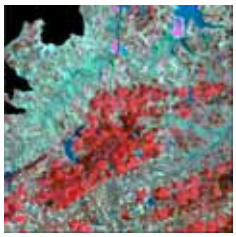

Figure 6. The color composite image of the study area

We applied the same UFCLS method in experiment 1 to process the data of the study area. Ten endmembers were extracted from the subscene. The classification image of vegetation, or the abundance fractions image of vegetation endmember, is presented in Fig.7. In the same way, we compare the classification image of vegetation with NDVI, shown in Fig.8. There are the same results with experiment 1. Furthermore, we find that the pixel classification image of vegetation agrees much more with the color composite image of raw bands 4, 3 and 2 in red, green and blue respectively in Fig.6, in which the red area generally denotes vegetation cover, than with the NDVI image. For example, the A region of rectangle in Fig.7 maybe had less vegetation than its surrounding region, which is seen clearly in Fig.6 than in Fig. 8. The B and C region of rectangle in Fig.7 are shown nearly in black, that indicates there were not vegetations in the regions, but in Fig.8 we can not find the result. The same regions are shown in close to turquoise in Fig.6. We know in this color composite image a

red region denotes vegetation cover, so it also indicates there were non-vegetation in the two regions.

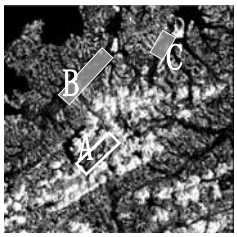


Figure 7. The classification image of vegetation

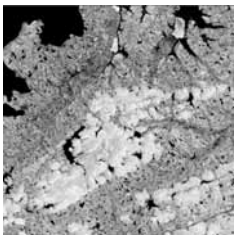

Figure 8. NDVI image

## 5. COMPARE UFCLS METHOD WITH CSMA

Constrained spectral mixture analysis (CSMA) was supposed by Liu Zhengkai et.al(1996). Using the CSMA algorithm, we can solve the linear spectral mixture model (1) through gradient iteration. For the two constraints, ASC and ANC, adding merit functions to the object function is applied in CSMA. So the constrained object function is defined as

$$\varepsilon=\|E\|^2+A_1g_1(F)+A_2g_2(F) \quad (8)$$

where $\|E\|^2$ denotes 2-norm in the error matrix E, i.e., the least squares error, and $g_1(F)$ and $g_2(F)$ are the merit functions of ASC and ANC respectively. Here $A_1$ and $A_2$ are constants; when they are given very large values, the minimum of ε is the minimum of $\|E\|^2$ under the two constraints of ASC and ANC. So the iterative equation is presented as follows

$$\alpha_n^{(k+1)}=\alpha_n^{(k)}-\delta\left(\frac{\partial\|E\|^2}{\partial\alpha_n}+A_1\frac{\partial g_1(F)}{\partial\alpha_n}+A_2\frac{\partial g_2(F)}{\partial\alpha_n}\right) \quad (9)$$

where $\alpha_n^{(k)}$ denotes the abundance fraction of the *n*-th endmember in the *k*-th iteration, and δ is the iterative step, which is generally given a small value in the range of 0 to 1.

We applied the CSMA method to estimate the abundance fractions of the six endmembers in the study area of experiment 1 (Fig.1). The classification result of the endmember $\mathbf{m_2}$ is presented in Fig.4(c). Compared it with NDVI (Fig.4(b)), it is shown that their similarities are not better than that of the $\mathbf{m_2}$ generated by UFCLS and NDVI, especially in the bottom of the image there are some distinct differences. And it did not classified the shade areas correctly as the UFCLS did, in Fig. 4(a) and 4(c) denoted by the circles.

Considering the consumption of the computing time, the UFCLS is also better than the CSMA. The latter consumed nine minutes to process the data of 51×51 pixels, but the former consumed less than one minute. The endmember signature matrix $\boldsymbol{M}$ is required when using the CSMA method, so it does nothing if the endmember signature matrix $\boldsymbol{M}$ is unknown. The values of the three parameters, δ, $A_1$ and $A_2$ in the equation (9), are obtained by repeating to do experiments, here $\delta=8\times10^{-8}/(3n+1)$, $A_1=6n\times10^5$ and $A_2=n\times10^4$. The $\mathbf{E}_L$ generated by the CSMA, i.e., the average value of relative error, defined by $\mathbf{E}_L=\frac{1}{n}\sum_{i=1}^{L}(E_i/D_{Ni})$, n denoting the total of spectral bands, was 18.5%, and that of the UFCLS was only 1.6%.

## 6. CONCLUSION AND DISCUSSION

The UFCLS method has been used for the inversion of linear spectral mixture model. The pixels classification was done through estimating the abundance fractions of endmembers. And the results indicated its effects are good. In our experiments the results of classification were verified only by the NDVI image, so the verification will be done by the measurement data of the land cover in the next study.

Compared the pixels classification results using the UFCLS with that of using the CSMA, it was shown that the former is better than the latter whether considering the effects of classification or the consumptive computing time. If the values of the three parameters, δ, $A_1$ and $A_2$ in the CSMA, are adjusted farther, the effects of classification will be improved and the consumptive time will be shorten. However, maybe this is just its disadvantage, because it is very difficult to find the proper values of these parameters.

The classification errors in the shade areas were increasing whether using the UFCLS or using the CSMA, which indicates the shade should be selected as an endmember in the inversion of the linear spectral mixture model.

## REFERENCES

Yingshi, ZH.,2001. A study on environmental change analysis in sand hill of Nebraska using remote sensing. *Geographical Research*, 20(2), pp. 213-219.

Shihao, T., Qijiang, ZH., Guangjian, Y., Xiaodong,, ZH., 2002. Effects of GA on the inversion of linear and nonlinear remote sensing models. *Journal of Beijing Normal University (Natural Science)*, 38(2), pp. 266-272.

Daniel, C. H., Chang, C. I.,2001. Fully constrained least squares linear spectral mixture analysis method for material quantification in Hyperspectral Imagery. *IEEE Transactions On Geoscience and Remote Sensing*, 39(3), pp. 529-545.

Bro, R., DE JONG S., 1997. A fast non-negativity-constrained least squares algorithm. *Journal of Chemometrics*, 11, pp. 393-401.

Daniel, C. H., Chang, C. I., 2000. Unsupervised fully constrained least squares linear spectral mixture analysis method for Multispectral Imagery. In: *Proceedings of IEEE 2000 International Geoscience and Remote Sensing Symposium*, Honolulu, USA, vol I-VI, pp. 1681-1683.

Zhengkai, L., Shuwei, C., 1996. Spectral mixture analysis of imaging spectrometer data. *Remote Sensing of Environment China*, 11(1), pp. 32-37.

## ACKNOWLEDGMENT

The authors would like to thank Jianxin MEI for his assistance with the computer program, and Lu ZHANG for providing the TM data. This work was supported by The National Key Basic Research and Development Program in China (2003CB415205).